NUCL SCI TECH (2022) 33:139
https://doi.org/10.1007/s41365-022-01123-w

Optimization study and design of scintillating fiber detector for D-T neutron measurements on EAST with Geant4

Wei-Kun Chen[1,2] · Li-Qun Hu[1] · Guo-Qiang Zhong[1,3] · Bing Hong[3] · Rui-Jie Zhou[1] · Kai Li[4] · Li Yang[1,2]

Received: 30 May 2022 / Revised: 16 September 2022 / Accepted: 17 September 2022 / Published online: 8 November 2022

Abstract Real-time monitoring of the 14-MeV D-T fusion neutron yield is urgently required for the triton burnup study on the Experimental Advanced Superconducting Tokamak (EAST). In this study, we developed an optimal design of a fast-neutron detector based on the scintillating fiber (Sci-Fi) to provide D-T neutron yield through Geant4 simulation. The effect on the detection performance is concerned when changing the number of the Sci-Fis embedded in the probe head, minimum distance between the fibers, length of the fibers, or substrate material of the probe head. The maximum number of scintillation photons generated by the n/γ source particles and output by the light guide within an event (event: the entire simulation process for one source particle) was used to quantify the n/γ resolution of the detector as the main basis. And the intrinsic detection efficiency was used as another evaluation criterion. The results demonstrate that the optimal design scheme is to use a 5 cm probe head whose substrate material is pure aluminum, in which 463 Sci-Fis with the same length of 5 cm are embedded, and the minimum distance between the centers of the two fibers is 2 mm. The optimized detector exhibits clear directionality in the simulation, which is in line with the expectation and experimental data provided in the literature. This study presents the variation trends of the performance of the Sci-Fi detector when its main parameters change, which is beneficial for the targeted design and optimization of the Sci-Fi detector used in a specific radiation environment.

Keywords Sci-Fi detector · Optimal design · n/γ resolution · Intrinsic detection efficiency · Geant4

1 Introduction

Using the 14-MeV fast neutrons generated by D-T fusion to study the triton burnup in deuterium plasma, and further study the behavior of alpha particles produced by the t(d, n)α fusion reaction is a commonly used method in tokamak experiments such as DIII-D [1, 2], FT [3, 4], TFTR [5, 6], JET [7, 8], ASDEX [9], and KSTAR [10–12]. Currently, among the existing D-T neutron measurement systems on the Experimental Advanced Superconducting Tokamak (EAST) [13], the neutron activation system (NAS) [14] can provide accurate D-T neutron yields without time resolution, and the 4H-SiC detector [15] is more suitable for extremely high neutron yields because of its small size and detection efficiency. Therefore, a new detection system with a higher detection efficiency for real-time monitoring of D-T neutrons is urgently required. Since a type of neutron detector based on the scintillating

This work was supported by the Users with Excellence Program of Hefei Science Center CAS (No. 2020HSC-UE012), the Comprehensive Research Facility for Fusion Technology Program of China (No. 2018-000052-73-01-001228), and the Institute of Energy, Hefei Comprehensive National Science Center (No. 21KZS205, 21KZL401).

✉ Guo-Qiang Zhong
gqzhong@ipp.ac.cn

[1] Institute of Plasma Physics, Hefei Institutes of Physical Science, Chinese Academy of Sciences, Hefei 230031, China

[2] University of Science and Technology of China, Hefei 230026, China

[3] Hefei Comprehensive National Science Center, Institute of Energy, Hefei 230031, China

[4] School of Mechanical and Vehicle Engineering, West Anhui University, Luan 237012, China

fiber (Sci-Fi) was developed by Los Alamos National Laboratory (LANL) in the 1990s, Sci-Fi detectors have been widely used for time-resolved 14-MeV neutron measurement on fusion devices such as TFTR [16], JT-60U [17], and LHD [18]. They are suitable for the study of time-resolved triton burnup owing to their fast response, high counting efficiency, gamma suppression capability, and directional response to incident neutrons [19–23]. The probe head mainly comprises the substrate material and embedded Sci-Fis. This structure provides a better n/γ resolution method than the traditional scintillation detector because the efficiency of energy deposition of incident neutrons and gamma-rays in Sci-Fis is different. Researchers have previously used Sci-Fi detectors to perform simple experimental comparisons, studying the effects of Sci-Fis of several different diameters and lengths on the performance of the detectors [23–25]. However, the results were not systematic because of the few samples with similar parameters. In addition, the same pure aluminum is usually selected as the substrate material of existing detectors because of its good shielding effect on β-rays, and there are few studies on the spacing of the Sci-Fis. Aiming at these aspects, this study tests several optimization directions for improving the performance of Sci-Fi detectors through simulations, and summarizes their effects.

The remainder of this paper is organized as follows. In Sect. 2, we describe the structure of the Sci-Fi detector and the principle of achieving n/γ resolution. Section 3 introduces the simulation conditions using Geant4 and the criteria for evaluating the design. In Sect. 4, the results of the simulations are explained in detail, including the possible reasons for the variation in the detection effect of each model on neutrons and gamma-rays. Section 5 concludes the paper and presents the final design scheme of the Sci-Fi detector suitable for use in the EAST device.

2 Structure and principle of Sci-Fi detector

The generally used structure of the Sci-Fi detector is shown in Fig. 1. Numerous dense and regularly arranged small holes are distributed in the cylindrical probe head, in which Sci-Fis are embedded and fixed. A light reflection layer can be placed in front of the probe to improve the utilization of scintillation photons. The rear of the probe head is directly connected to a photomultiplier tube (PMT) or connected through a light guide to adjust the light path. When the diameter of the probe head does not match the PMT, the tapered light guide can first collect the scintillation photons generated in all the fibers and thereafter focus on the photocathode of the PMT [24]. In addition, to avoid the effects of electromagnetic pulses (EMPs), optical

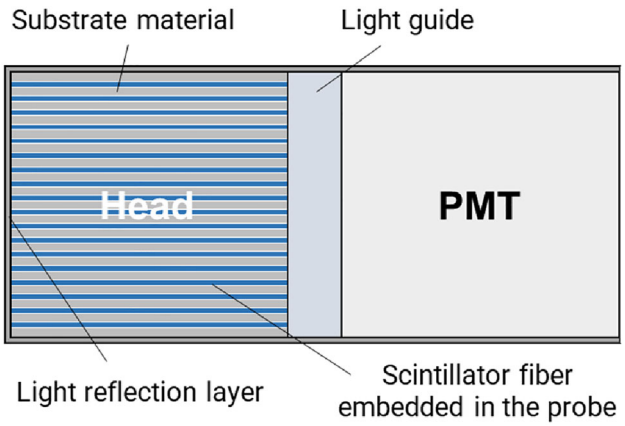

Fig. 1 (Color online) Structure of the Sci-Fi detector

fibers with low transmission attenuation can optionally be used to transfer scintillation photons to the PMT which is located far away from the EMP source and shielded well [26].

The particles that enter the probe head and deposit energy at the core of the Sci-Fis will cause the generation of scintillation photons. When reaching the end of the fiber, these photons are either directly output or first collected by the light guide and then output to the photocathode of the PMT, where a pulse signal is finally formed. This process completes in less than 1 μs, resulting in a fast response of the Sci-Fi detector. For incident neutrons, they are scattered within the Sci-Fis that are made of hydric materials, and recoil protons are generated. Note that the latter have a large energy loss per unit pathlength (dE/dx); thus, they can generally deposit most of their energy into the fibers, emitting numerous scintillation photons in this process. In contrast, for incident gamma-rays, the energy is mainly deposited into the fibers through the Compton and electron pair effects, generating electrons and positrons. These electrons and positrons can easily escape from the fiber, because the electron trajectories are not strait like random walk. In addition, secondary electrons have a much longer range than protons; thus, they typically deposit only a small amount of energy before leaving the first fiber where they are born and entering the substrate of the probe head. At this point, the substrate of the low-Z material can act as a shield to prevent them from entering other adjacent fibers, thereby avoiding the extra energy deposition and generation of scintillation photons. This implies that the recoil protons produced by incident neutrons are much more efficient in depositing energy in Sci-Fis than the secondary electrons produced by gamma-rays. Therefore, there is a large difference in the number of scintillation photons that can be generated in the fibers by incident neutrons and gamma-rays, which also implies that a threshold can be set to achieve the n/γ resolution. Similarly, regardless of the

incident angle, the energy of the recoil proton is determined by the incident neutron energy; thus, the energy resolution of the neutrons can also be achieved by setting an appropriate threshold.

3 Simulation and evaluation criteria

Currently, Monte Carlo method is widely used to optimize the design of new detectors and test the performance of detectors which are affected by different measurement conditions [27–29]. In this study, Geant4 (version 10.06.p02) was used for the Monte Carlo simulations [30]. We selected QGSP_BIC_HP [31] as the physical list in the simulation process, which defines the physical laws obeyed by all the interaction processes that occur inside the model. It contains hadronic, electromagnetic, and decay components. In addition, it uses high-precision neutron models and cross sections to describe elastic and inelastic scattering, capture, and fission for neutrons below 20 MeV. To ensure that all scintillation photons could be properly generated, reflected, attenuated, and absorbed, the original physics list was replaced with G4EmStandardPhysics_option4, thereby adding the physics of optics to the simulation process [32].

3.1 Source particles and simulation models

During the simulations of the two source particles, 14-MeV D-T fusion neutrons and 15-MeV gamma-rays were selected for use. The choice of gamma-rays energies considers the following factors: the numerous hard X-rays produced by bremsstrahlung from collisions of run-away electrons with other particles or the walls of the vacuum chamber during D-D fusion experiments in large tokamak devices, and gamma-rays from various nuclear reactions in plasmas. The energies of these X/γ-rays can reach the MeV range, and their distribution exceeding 8 MeV can still be observed in the EAST tokamak [33]. They significantly interfere with the neutron detection of traditional scintillation detectors, whereas the structure of the Sci-Fi detector can eliminate the influence of lower-energy X/γ-rays. However, for high-energy X/γ rays above 10 MeV, the energy deposition in the fibers is close to the energy deposition of D-T fusion neutrons. Although these high-energy X/γ-rays are rare, their influence cannot be ignored because of the also low D-T neutron yield. Considering the experimental requirements of higher plasma temperature and density in future at EAST, 15-MeV gamma-rays were used as the source particle to evaluate the response of the Sci-Fi detector to gamma-rays. During the simulations, both neutron and gamma-ray particle sources were isotropic point sources placed 50 cm in front of the axial center of the probe head. The number of source particles per simulation was set as 2×10^8.

For the new Sci-Fi detector designed in this study, the basically same structure as Fig. 1 was adopted. The model of the Sci-Fi embedded in the probe head was constructed with reference to the Sci-Fi: Kuraray SCSF-78 M [34], as shown in Fig. 2. It has the commonly used diameter of several Sci-Fi detectors, which is 1 mm [19–21, 35, 36], and a double cladding structure. The thickness of each cladding is 3% of the light diameter. The effective attenuation length of the fiber core for scintillation photons was determined according to [37]. In addition, several of the same materials in the wavelength-shifting fiber (wls), which is one of the basic example files provided in Geant4, were also used as references when selecting other parameters. Note that the fibers were multi-stacked in a trefoil shape to ensure a uniform and dense distribution. The Sci-Fis were arranged from the inside to the outside. This implies that the added fibers will be supplemented to the insufficient part of the inner layer and thereafter automatically set to the outer layer when the inner layer is full. Immediately behind the probe head, a 10-mm-thick polymethyl methacrylate (PMMA) light guide was used as a collection and counting container for all scintillation photons generated in the fibers. The diameter was the same as that of the probe head. The number of photons output by the light guide was focused. A tubular aluminum shell with a thickness of 1 mm completely covered the side of the cylindrical probe head and light guide, and a light reflection layer was arranged in front of the probe to improve the utilization efficiency of scintillation photons. The interface between the core layer and cladding layers of the Sci-Fis, fibers and light guide, fibers and probe head substrate, and finally, light guide and substrate were set as optical boundary layers to reduce the leakage of photons. The PMT was not simulated because the reaction that occurs when the photons reach the photocathode is already known, and the amplitude of the final output signal is nearly linear with the number of scintillation photons. Therefore, we directly used the number of scintillation photons output by the light guide to characterize the output signal amplitude of the Sci-Fi detector in the theoretical case.

To reduce electromagnetic interference during experiments on EAST in actual use, the detector is usually placed in a magnetic shielding tube made of permalloy. Accordingly, the effect of the shielding tube was considered in the simulation. The tube used for each simulation had a total length of 32 cm, including the front and back covers. The thickness of the tube was all 1 cm, but its inner diameter was adjusted with the diameter of the probe and a gap of 5 mm was maintained from the probe head.

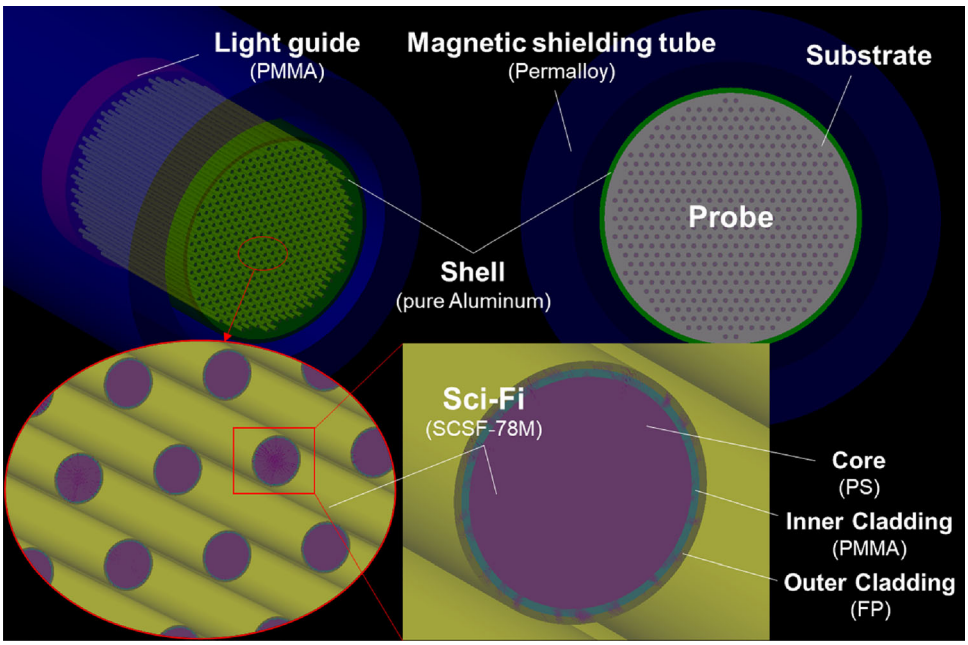

Fig. 2 (Color online) One of the Geant4 simulation models used in this study. The aluminum shell in front of the probe was set as the light reflection layer

3.2 Design optimization and evaluation criteria

Four optimization directions were selected when establishing the probe models: the optimum number of the Sci-Fis embedded in the probe head, optimum distance between the fibers, length of the fibers, and probe head substrate materials. Pure aluminum was used as the substrate material for the first three sets of simulations, and a PMMA-based probe was simulated for comparison. The four parameters used in the Sci-Fi detectors are closely related to the detection efficiency. However, considering that the volume and cost of the detector must be controlled within a certain range, the intrinsic detection efficiency (IDE) of the detector was selected as another reference factor for evaluating the detector performance, in addition to the ratio of the highest n/γ pulse signal amplitude (n/γ ratio). In this study, the n/γ ratio was determined using the following formula:

$$\mathrm{n}/\gamma\,\mathrm{ratio} = \frac{N_{\mathrm{out,n,max}}}{N_{\mathrm{out},\gamma,\mathrm{max}}},$$

where $N_{\mathrm{out,n,max}}$ denotes the maximum count of scintillation photons emitted from the end of the light guide in an event (event: the entire simulation process for one source particle) when the source particle is a neutron, and $N_{\mathrm{out},\gamma,\mathrm{max}}$ denotes the case when a gamma-ray source is used.

The calculation formula of the IDE was set as follows:

$$\mathrm{IDE} = \frac{N_{\mathrm{eff}}}{N_{\mathrm{in}}} = \frac{N_{\mathrm{out}}}{N_{\mathrm{in.fib}} + N_{\mathrm{in.sub}}},$$

where N_{eff} denotes the number of events that generate the output signal; N_{in} denotes the number of events with source particles entering the probe head; N_{out} denotes the number of events with photons exiting from the end of the light guide; and $N_{\mathrm{in.fib}}$ and $N_{\mathrm{in.sub}}$ denote the number of events in which particles have entered the Sci-Fis and the number of events in which the particles only enter the probe head substrate and do not enter the fibers, respectively. Moreover, $N_{\mathrm{in.fib}}$ can be divided into two parts: the number of events with source particles depositing energy in the fibers ($N_{\mathrm{in.fib.eff}}$) and without energy deposition of source particles in the fibers ($N_{\mathrm{in.fib.ineff}}$).

4 Results and discussion

4.1 Effect of the number of Sci-Fis

For the simulations described in this section, we constructed eight models using different numbers of Sci-Fis. Under the condition that the distance between the outermost Sci-Fi and the side edge of the probe head was the same, we selected the minimum number of fibers as 73 and the maximum as 979. The diameter of the probe head ranged from 20.4 to 68.8 mm, with a minimum distance of 2 mm between the centers of the two fibers. Therefore, the minimum thickness of the substrate between the fibers was 1 mm, which is a commonly used parameter for Sci-Fi detectors [24]. For the same reason, the lengths of the probe head and Sci-Fis were set to 5 cm. Taking the simulation results of the model constructed with 463 Sci-Fis as

an example, the obtained output photon number spectra are shown in Fig. 3. It should be noted that, for the reason explained in Sect. 3, the number of photons output in an event represents the pulse height of the complete detector's output signal; thus, Fig. 3 can also be considered as the pulse height spectra of the detector with 463 Sci-Fis when detecting 14-MeV neutrons and 15-MeV gamma-rays. The intersections of the four curves and the horizontal axis represent not only the maximum number of photons output by the light guide in an event, but also the maximum amplitude of the pulse output by the complete Sci-Fi detector.

Figure 3 shows that the probe using pure aluminum as the head substrate material is more efficient in outputting photons than the PMMA-based probe when the source particles are either neutrons or gamma-rays. This is because the probes of the two head substrates have different types of optical boundary layers between the fibers and substrate, resulting in different photon transmission efficiencies. Meanwhile, it can be observed that, when 14-MeV neutrons are incident, the maximum number of output photons in an event is greater than the case when the incident particles are 15-MeV gamma-rays. This proves that the Sci-Fi detector has a good n/γ resolution capability because researchers can screen out D-T neutrons by selecting the n/γ boundary reasonably on the energy spectrum. In this study, we verified the reason for this phenomenon through simulation. Figure 4a shows the distribution of the initial energies of the recoil protons produced by incident neutrons and electrons produced by incident gamma-rays in the Sci-Fis. Considering that incident particles within an event may generate secondary particles in multiple fibers, we counted the accumulation in all the fibers. Figure 4b shows the distribution of energy deposition of these secondary particles in the fibers. Although the highest energy of recoil protons generated by incident neutrons is lower than that of secondary electrons generated by gamma-rays, the former can deposit more energy in Sci-Fis. This demonstrates that neutrons are more efficient at depositing energy in the Sci-Fi detector, thus generating more scintillation photons and achieving n/γ resolution. In addition, the two curves of the Al-based probe are farther apart on the horizontal axis in Fig. 3, indicating that the Al-based probe has better n/γ resolution than the PMMA-based probe when using 463 Sci-Fis.

In addition, the counts in Fig. 3 are concentrated in the regions where the number of output photons is low. This makes the counts at the intersections of the four curves and the horizontal axis excessively few to ensure the accuracy of the calculated n/γ ratio; therefore, we selected a higher count as the location of the horizontal baseline to reduce accidental errors. Meanwhile, the spectra were smoothed based on the CERN ROOT framework [38] to reduce the subjective errors.

The relationship between the number of the Sci-Fis used in the probe head, n/γ ratio, and IDE is shown in Fig. 5. Figure 5a shows that increasing the number of fibers in the Al-based probe is beneficial to n/γ resolution, but the effect is close to the upper limit when the number of fibers is 463. In contrast, the PMMA-based probe is not sensitive to the number of Sci-Fis used in it. In Fig. 5b, it can be seen that the IDE of the detector also increases but has an upper limit when more fibers are used, which may be due to the self-shielding of the isotropic point source by the probe. When

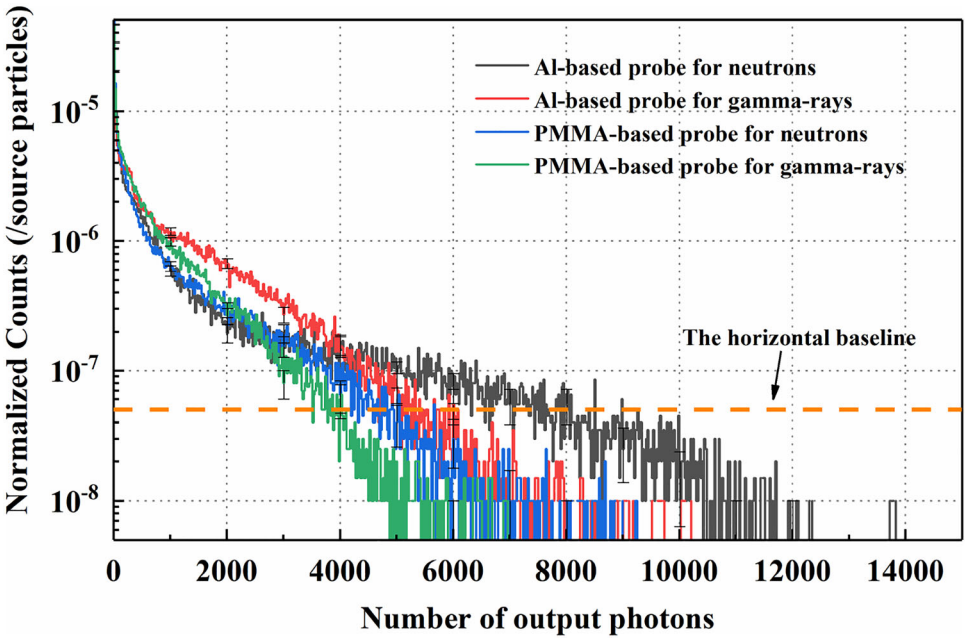

Fig. 3 (Color online) Spectra of the photon number output by the light guide in an event when simulated using a model with 463 Sci-Fis embedded in the probe head. The counts have been normalized to each source particle

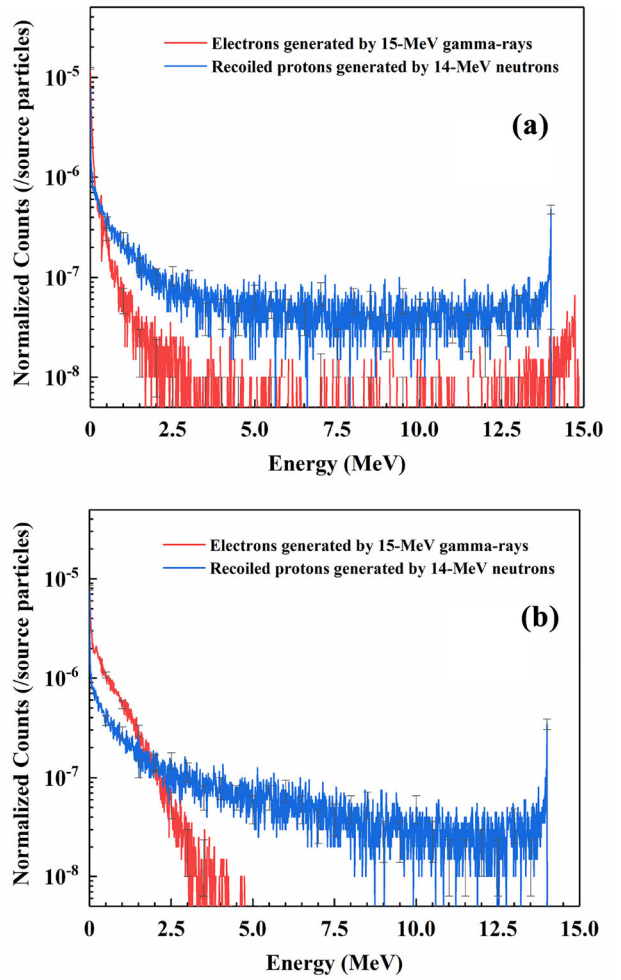

Fig. 4 (Color online) Distributions of **a** the total initial energy in an event and **b** the total energy deposition in an event of recoil protons and electrons when the source particles are 14-MeV neutrons and 15-MeV gamma-rays, respectively. These two results are based on a model using 463 Sci-Fis embedded in the probe head. The counts have been normalized to each source particle

the number of Sci-Fis is increased, the newly added fibers are placed on the periphery of the probe head, and thus the self-shielding effect is enhanced, which offsets the increase in detection efficiency. In addition, for the two probes using the two head substrate materials, the number of events with source particles entering the probe head (N_{in}) is not significantly different, but the IDE for neutrons of the PMMA-based probe is significantly higher than that of the Al-based probe. This may be related to the interaction of neutrons with these two substrate materials, because incident neutrons generate recoil protons more efficiently in the PMMA substrate, but generate gamma-rays and secondary electrons more efficiently in the substrate of pure aluminum, which is consistent with the particle species and numbers that we have recorded. This can be explained as follows.

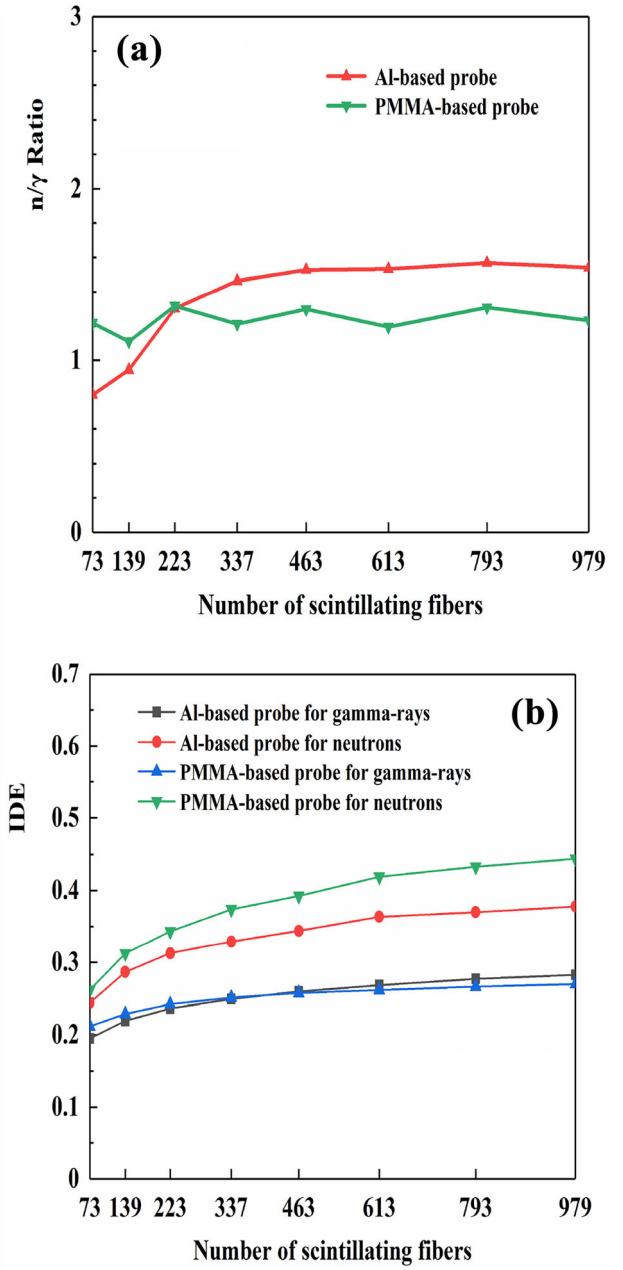

Fig. 5 (Color online) Variation trends of **a** n/γ ratio and **b** IDE of Sci-Fi detectors affected by the number of Sci-Fis embedded in the probe head

(1) When the source particles are neutrons, the proportion of $N_{in.fib}$ in N_{in} of the PMMA-based probe is much higher than that of the Al-based probe. Furthermore, a large increase in the number of protons is observed in the fibers of the former, whereas the total energy deposition of protons does not change significantly. Therefore, it can be speculated that numerous recoil protons are generated in the PMMA substrate. Some of them and scattered neutrons subsequently enter the fibers and deposit

energy, leading to an increase in N_{out} and the IDE of the PMMA-based probe compared with those of the Al-based probe.

(2) In contrast, when neutrons are incident, gamma-rays are abundantly generated in the pure aluminum substrate, which is also consistent with the fact that the number of gamma-rays and electrons in the fibers of the Al-based probe is higher. It can be speculated that numerous secondary electrons are generated in the aluminum substrate, and some of them and gamma-rays subsequently enter the fibers. However, because electrons deposit energy much less efficiently than protons, these extra electrons and gamma-rays have little effect on N_{out} and the IDE.

In summary, the Sci-Fi detector using the PMMA-based probe head has a higher IDE for neutrons, but these extra neutrons and recoil protons recorded in Sci-Fis have little effect on the n/γ resolution because some of their energy has been lost in the substrate. Note that the IDE for gamma-rays is not significantly different between the probes of the two substrate materials, because both low-Z materials are insensitive to gamma-rays (Fig. 5b). In conclusion, according to the results shown in Fig. 5, when the length of the probe head and fibers is 5 cm and the minimum distance between the centers of the two fibers is 2 mm, the Al-based probe using 463 fibers is the most cost-effective design. Using fewer fibers will cause the detector's n/γ resolution and IDE to decrease, while using more fibers cannot significantly improve the detector's n/γ resolution. However, to design a smaller probe with fewer Sci-Fis, it may be better to select PMMA as the substrate material of the probe head.

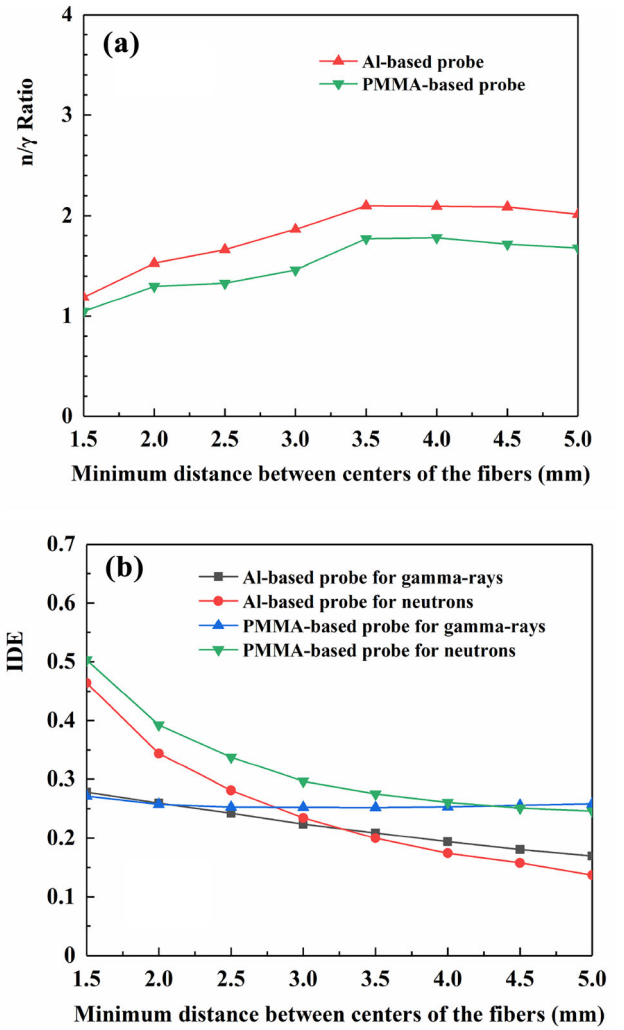

Fig. 6 (Color online) Variation trends of **a** n/γ ratio and **b** IDE of Sci-Fi detectors affected by the minimum distance between the centers of the two fibers embedded in the probe head

4.2 Effect of the minimum distance between Sci-Fis

Under the condition that the number of Sci-Fis is 463, the effect of changing the minimum spacing between fibers on the n/γ resolution and IDE of the detector could be simulated. Considering that the diameter of the fibers is 1 mm, the selection of the minimum distance between the centers of the two fibers started from 1.5 mm; thus, the minimum thickness of the substrate between the fibers was 0.5 mm in this case.

Figure 6a shows the effect of fiber spacing on the n/γ ratio of the probe. Considering that the recoil protons generated by neutrons in Sci-Fis have an extremely short range and large energy loss per unit pathlength (dE/dx), they are easily absorbed by the fiber itself. For protons to escape from the fiber, a thin layer of substrate material can provide a good shielding effect. In contrast, for gamma-rays, the secondary electrons and positrons generated in the fibers are more likely to escape into the adjacent fibers and deposit extra energy. Among them, the low-energy electrons and positrons can be well shielded by the 1-mm substrate material; however, the higher-energy electrons, which may affect the n/γ ratio, must be effectively blocked by increasing the thickness of the substrate between the fibers. Note that as the distance between the fibers increases, the self-shielding of the source particles by the probe is also enhanced. It is disadvantageous that neutrons are shielded more strongly owing to the small Z-value of the substrate material. Therefore, it can be observed that both curves in Fig. 6a have a turning point. When the minimum distance between the centers of the two fibers is less than 3.5 mm, the increase in the substrate thickness is favorable for the n/γ ratio of the probe. However, when the distance is greater than 3.5 mm, the number of secondary electrons that escape to adjacent fibers is reduced to an extremely low level, whereas self-shielding by the probe is

enhanced to become the dominant factor affecting the n/γ ratio. Therefore, a minimum distance between the fibers greater than 3.5 mm adversely affects the n/γ ratio. It should be emphasized that if the energy of the gamma-rays in the environment is lower than 15 MeV, the position of this turning point will correspondingly advance.

In addition, an increase in this minimum distance leads to a decrease in the IDE, as shown in Fig. 6b. This is easy to understand because the sensitive volume of the probe head does not change, but the overall volume increases. Based on the aforementioned reasons, and considering that the newly designed detector is as small as possible to meet the requirements of the narrow space around the EAST device, we still selected 2 mm as the minimum distance between the centers of the two Sci-Fis. The diameter of the probe head in this case was 48 mm, which is in good agreement with the size of a 2-inch PMT, thus avoiding the photon loss caused by the use of a tapered light guide.

4.3 Effect of the length of Sci-Fis

The length of the Sci-Fis used in the Sci-Fi detector is usually the same as that of the probe head, which is generally in the range of 5–20 cm. In this simulation, the lengths of the two were also equal, and eight models with different fiber lengths were tested. To examine the case of the shorter probe and Sci-Fis, the length was set to a minimum of 2.5 cm and increased at 2.5 cm intervals. The results are shown in Fig. 7. It should be noted that there may be large errors in the Al-based probe data at a length of 2.5 cm. The reasons for this are as follows.

Taking Fig. 8 as an example, because we set the counting threshold (the position of the horizontal baseline) to reduce accidental errors when calculating the n/γ ratio, part of the data will be lost. When the length of the probe head is excessively short (2.5 cm), the IDE of the Sci-Fi detector is extremely low; therefore, it may not produce sufficient counts. In comparison with gamma-rays, the data points of neutrons are more scattered and the curve is flatter, which is more affected by the threshold, resulting that the calculated n/γ ratio is lower than expected. In contrast, the PMMA-based probe is slightly less affected owing to more concentrated counts and a higher IDE, compared with the Al-based probe. Therefore, according to the trend of the curves of the PMMA-based probe shown in Fig. 7a, it can be inferred that, if the statistical counts are sufficient, the revised curve of the Al-based probe should theoretically be decreased before the length is taken as 5 cm.

In addition, the length of the probe head significantly affects its self-shielding effect. As shown in Fig. 8, when the probe head length increases, the maximum value of the abscissa of the four curves, particularly the curve

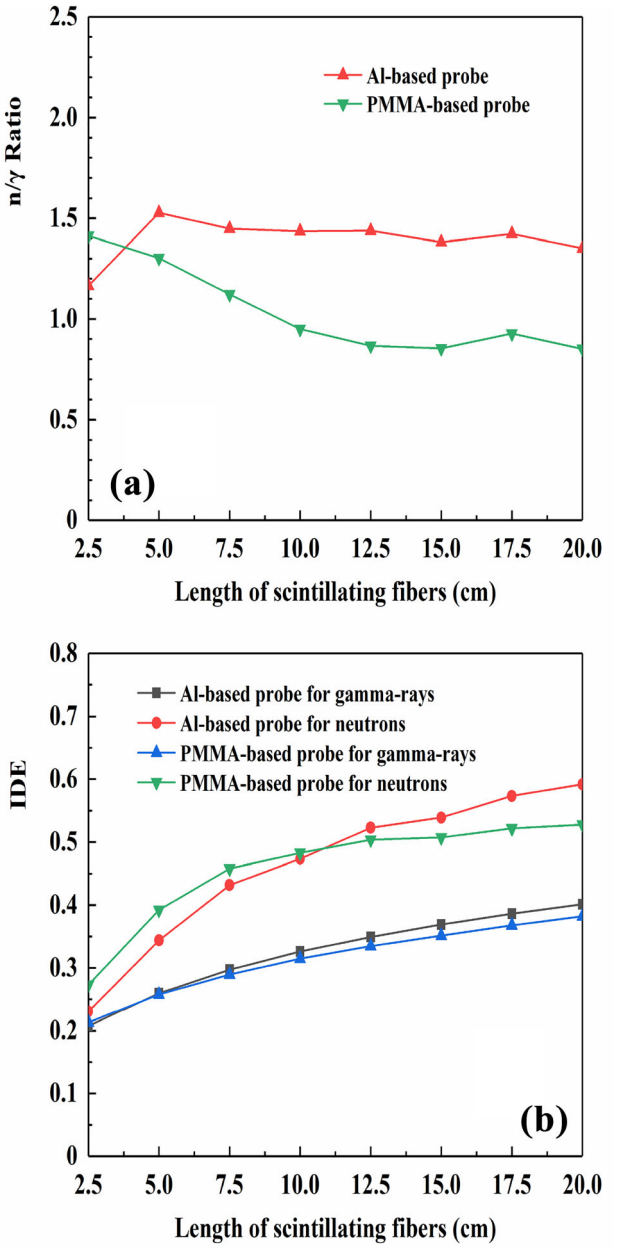

Fig. 7 (Color online) Variation trends of **a** n/γ ratio and **b** IDE of Sci-Fi detectors affected by the length of Sci-Fis and probe head

representing neutrons, decreases, and upward bulges appear in the middle of the curves. The reasons for this are as follows.

(1) Limited by the effective attenuation length of the Sci-Fis to photons, when the length of the fibers and the probe head increases, only a few scintillation photons generated in the front of the fibers can reach the light guide with suitable emission angles, and other photons are lost during the transmission process. These angles must satisfy the requirement that the photons can be totally reflected at the fiber

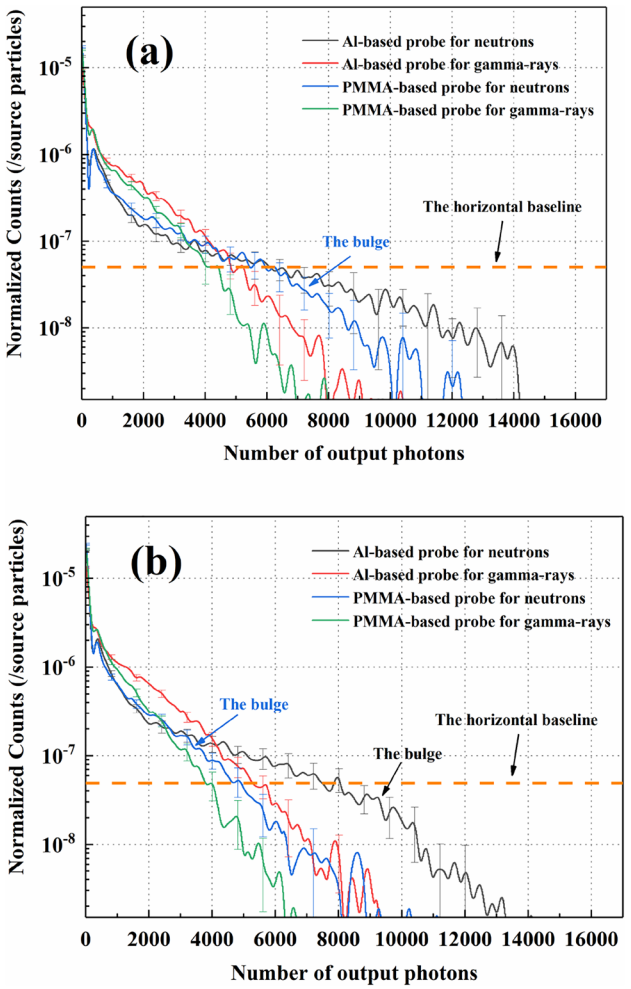

Fig. 8 (Color online) Spectra of the number of photons output by the light guide within an event when simulated using a model of **a** a 2.5-cm probe head and **b** a 5-cm probe head. The counts of both subfigures have been normalized to each source particle and all curves have been smoothed based on the CERN ROOT framework

boundary, and should be as consistent as possible with the axis of the fiber. Because only the photon is rarely reflected, the distance from its generation to entry into the light guide can be shortened to reduce the probability of absorption. Therefore, except in cases where the length of the probe head is extremely short, the scintillation photons generated in the fibers at positions far from the light guide cannot generally be fully recorded. Reflecting on the photon number spectrum output by the light guide, it means that when incident particles deposit energy in the front of the fibers, they can only generate fewer photons than the theoretical value in an event, which causes the spectral curve to shift to the left.

(2) The scintillation photons generated close to the light guide are less affected by scattering and absorption during transmission; therefore, their numbers can better reflect the energy of the incident particles. Accordingly, the rightmost positions on the horizontal axis that the curves can reach in Fig. 8a and b are determined by the energies of the incident particles that can reach positions close to the light guide in the fibers. However, the energy of the incident particles, particularly neutrons, decreases during their flight inside the probe head owing to the self-shielding effect. Consequently, the energy deposited by the incident particles and the number of photons generated in fibers at positions close to the light guide are reduced, which also causes the spectral curve to shift to the left.

In conclusion, the enhancement of the self-shielding effect caused by increasing the probe head length is detrimental to the n/γ resolution of the detector. The PMMA-based probe causes a stronger neutron self-shielding effect because of the smaller Z-value of its substrate material; therefore, the bulge on the curve appears when the probe head length is only 2.5 cm, while this length is 5 cm for the Al-based probe. It can be speculated that, for Sci-Fi detectors that generally use low-Z materials as the probe head substrate, the probe head and Sci-Fis embedded in it should not be too long. Additionally, Fig. 7b shows that the IDE of the detector increases with the length of the probe head. This may also result from the self-shielding effect by the probe. The extra part of N_{out} is due to the source particles scattered by the substrate; however, it is useless for counting the maximum number of photons in an event because the energy of the source particles has already been partially lost in the substrate. PMMA has a better neutron moderation effect than pure aluminum, which may explain why the IDE of the Al-based probe exceeds that of the PMMA-based probe when the length is greater than 11 cm. In addition, it can be predicted from Fig. 7b that the curves representing the IDE all have an upper limit, which may be related to the attenuation of scintillation photons as they travel through the fibers. Considering all this, it is appropriate to use 5 cm as the length of the probe head and Sci-Fis.

4.4 Effect of the substrate material of the probe head

The selection of the substrate material should consider the following key points:

(1) It should have a strong shielding effect on recoil protons and β-rays.
(2) When it shields protons and β-rays, the bremsstrahlung radiation should be as low as possible.
(3) Because of the dense distribution of Sci-Fis inside, the interaction of the substrate with incident neutrons

and gamma-rays should not generate excess secondary particles.

In the previous sections, we analyzed the simulation results using pure aluminum, which is a light metal material, and PMMA, which is a light non-metal material, as the probe head substrate. Among them, PMMA is an emitter of recoil protons, which was only used as a reference in this study and has been proven to be unsuitable as a substrate material in most cases. Considering the lower material densities of aluminum and PMMA, shielding the secondary particles generated in fibers is disadvantageous. Therefore, we conducted supplementary experiments focusing on simulating the effect of using stainless steel (SUS304, a medium-quality metal) and lead (a heavy metal) as substrate materials. The case of a Be-based probe was also simulated as a reference for metal substrate materials lighter than aluminum.

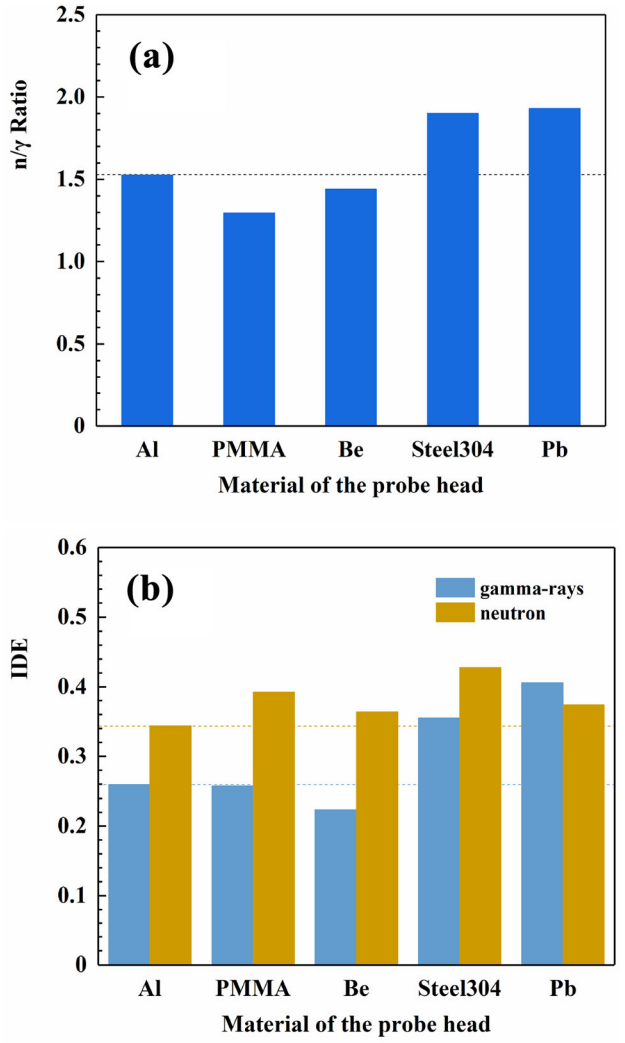

Fig. 9 (Color online) **a** n/γ ratio and **b** IDE of Sci-Fi detectors affected by the substrate material of the probe head

Figure 9 shows the simulation results, which are consistent with our expectations. It can be seen that, as the material density increases, the n/γ resolution of the detector increases significantly. Because lead has a larger density and larger absorption cross sections for gamma-rays, the detector designed with it as the substrate material has the strongest suppression ability for gamma-rays; thus, it has the highest n/γ ratio. However, as shown in Fig. 9b, the IDEs of the detectors made of these five substrate materials are significantly different. Among them, the IDE of incident gamma-rays clearly increases with the increase in the Z-value of the substrate material, which may be due to the influence of bremsstrahlung. Our analysis of the data reveals that the major factor affecting the IDE is the change in N_{out}. To clarify this, we measured the energy deposition in Sci-Fis of several major secondary particles directly generated by the source particles when different substrate materials were used. Tables 1 and 2 list the cases in which the incident particles are neutrons and gamma-rays, respectively. Ideally, the lower the number and energy deposition of these secondary particles in the fibers, the stronger the shielding effect of the substrate and the less the substrate interferes with neutron detection. This is because secondary particles from adjacent fibers or the substrate are undesirable and should be avoided to deposit energy in the next fiber.

From Tables 1 and 2:

1. As a proton emitter under fast-neutron irradiation, PMMA has a significant adverse effect on neutron detection. However, the advantage is that it is not sensitive to gamma-rays.
2. Beryllium is ideal for use as the substrate material, because it is not easy to generate interfering particles. However, considering the toxicity of its metal and compounds, it is not actually suitable for use.
3. Steel304 and lead have higher *Z*-values, which promote strong Compton scattering and electron pair effect of gamma-rays in the substrate. Although the generated electrons and positrons are not high in energy, they are in large quantities and appear inside the detector, which easily cause the accumulation of signals and saturation of counting. In addition, Table 1 shows that they rarely generate recoil protons that affect neutron detection; however, protons exiting the fibers generate strong bremsstrahlung in the substrate. This may explain why detectors based on these two materials have a higher IDE for neutrons, as shown in Fig. 9b.
4. The aluminum substrate is not excessively sensitive to incident neutrons and gamma-rays, which can better satisfy the requirements of suppressing gamma-rays without hindering neutron detection.

Table 1 Total energy deposition in the Sci-Fis of protons and electrons directly generated by the source neutrons

		Al	PMMA	Be	Steel304	Pb
Proton	E_{dep} (MeV)	76,094.9	89,602.1	77,647.4	71,977.5	75,065.9
	Count	14,373	32,161	14,833	13,565	14,172
e^-	E_{dep} (MeV)	0	0	0	55.75	0
	Count	0	0	0	148	0

Table 2 Total energy deposition in the Sci-Fis of electrons and positrons directly generated by the source gamma-rays

		Al	PMMA	Be	Steel304	Pb
e^-	E_{dep} (MeV)	17,701.2	15,511	16,113.1	17,595.1	17,609
	Count	23,456	17,679	17,892	36,218	39,455
e^+	E_{dep} (MeV)	7042.95	4795.09	5538.7	8573.98	11,964.7
	Count	10,774	6644	7154	19,959	30,155

In view of the above considerations, pure aluminum is more suitable to be used as the substrate material for Sci-Fi detectors because of its good n/γ resolution and insensitivity to both neutrons and gamma-rays. Pb-based probes are also a good choice if the gamma-rays are of low intensity or have been shielded in the detector's operating environment.

4.5 Directionality of the optimized Sci-Fi detector model

Directionality is one of the most important characteristics of the Sci-Fi detector. For the optimized design (5 cm Al-based probe head, with 463 Sci-Fis spaced 2 mm apart embedded in it), we investigated the response of the detector to particle sources at different angles.

Figure 10 verifies the directionality of the Sci-Fi detector. Compared with the particle source on the side, the particles incident on the front (0°) can generate more scintillation photons in the fibers, implying that the detector can output higher pulse signals. Figure 10a shows that the height difference between the highest signal generated by 0°–90° incident neutrons is only approximately 20%, because a higher baseline position was selected to ensure the reliability of the data (Fig. 3). Figure 10b shows the counts of the signals generated in the detector according to the thresholds of different signal heights when using the statistical method used in [24]. This method uses all counts and can observe the relatively apparent directionality of the Sci-Fi detector. It should be noted that:

(1) Source particles incident at 0° have an advantage in depositing energy in the fibers. However, for the reasons explained in Sect. 4.3, it may be offset by the self-shielding effect by the probe and the optical attenuation in the fibers.

(2) The magnetic shielding tube in the model may adversely affect the directionality of the detector.

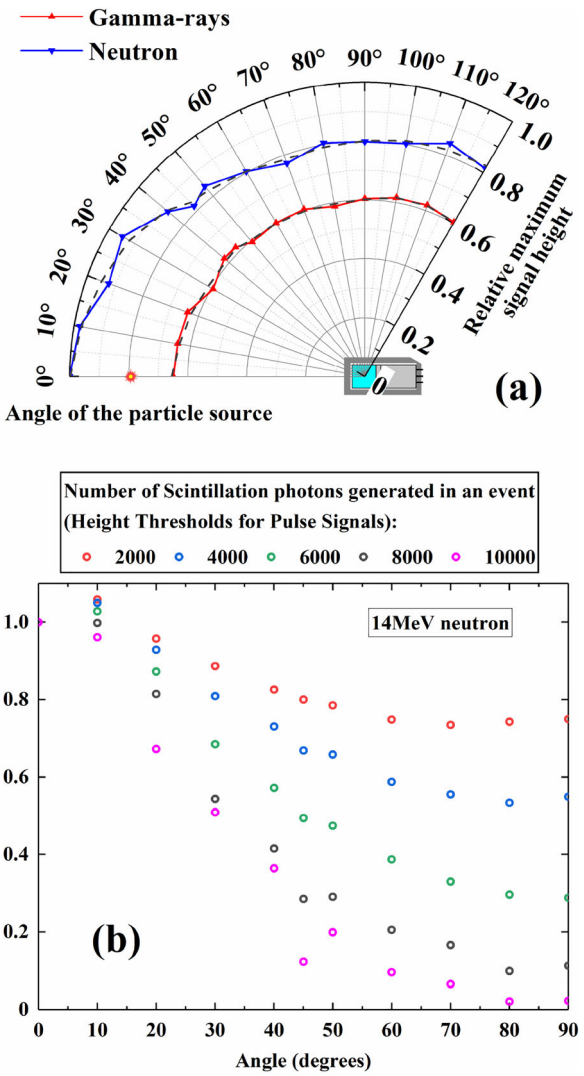

Fig. 10 (Color online) **a** Relative maximum signal height and **b** relative counts of signals at different heights when the particle source is at different angles to the detector. Note that the signal height is represented by the number of scintillation photons output by the light guide within an event

Compared with neutrons, the Sci-Fi detector is less affected by the incident angle of the particles when measuring gamma-rays; therefore, the n/γ resolution worsens with the increase in the incident angle. This implies that the angle to the source must be considered when using the Sci-Fi detector.

5 Conclusion

To design optimal Sci-Fi detectors to provide time-resolved triton burnup of the plasma in the experiments on EAST, several sets of simulation experiments have been carried out. Besides the type and parameters of the Sci-Fis that are used, the number of the fibers embedded in the probe head, minimum distance between the fibers, length of the fibers, and substrate material of the probe head are the main factors that can affect the performance of the detector. The n/γ resolution capability is the key guarantee for the Sci-Fi detector to accurately measure 14-MeV D-T fusion neutrons; therefore, it is used as the main basis to evaluate the design scheme. In addition, considering the limitations of the manufacturing cost and volume, the IDE of the detector is also taken as a reference. The results demonstrate that the optimal design scheme is to use a 5-cm probe head whose substrate material is pure aluminum, in which 463 Sci-Fis with the same length of 5 cm are embedded, and the minimum distance between the centers of the two fibers is 2 mm. The optimized detector exhibits clear directionality in the simulation, which is in line with the expectation and experimental data provided in the literature. It should be emphasized that the self-shielding by the probe is an important factor affecting the n/γ resolution of the Sci-Fi detector. In addition, multiple simulation results in this study implied that reducing the loss of scintillation photons in the fibers during transmission significantly impacts the detector performance; therefore, the Sci-Fis embedded in the probe head must be carefully selected. The information presented in this paper will be beneficial for designing Sci-Fi detectors with higher cost-effectiveness and better D-T neutron screening capability for different radiation environments in future.

Author contributions All authors contributed to the study conception and design. Material preparation, data collection and analysis were performed by Wei-Kun Chen, Li-Qun Hu, Guo-Qiang Zhong, Bing Hong, Rui-Jie Zhou, Kai Li, and Li Yang. The first draft of the manuscript was written by Wei-Kun Chen, and all authors commented on previous versions of the manuscript. All authors read and approved the final manuscript.

References

1. J.R. Smith, R.K. Fisher, J.S. Leffler et al., Time- resolved 14-MeV neutron detector for triton confinement studies. Rev. Sci. Instrum. **57**, 1780–1782 (1986). https://doi.org/10.1063/1.1139180
2. H.H. Duong, W.W. Heidbrink, Confinement of fusion produced MeV ions in the DIII-D tokamak. Nucl. Fusion **33**, 211–224 (1993). https://doi.org/10.1088/0029-5515/33/2/i03
3. P. Batistoni, M. Martone, M. Pillon et al., Measurements of triton burnup in low Q discharges in the FT tokamak. Nucl. Fusion **27**, 1040–1043 (1987). https://doi.org/10.1088/0029-5515/27/6/017
4. P. Batistoni, E. Bittoni, M. Haegi, Triton confinement as inferred from fusion produced neutron measurements in the FT tokamak. Nucl. Fusion **29**, 673–679 (1989). https://doi.org/10.1088/0029-5515/29/4/011
5. J.S. McCauley, J.D. Strachan, Measurement of DT neutron emission from TFTR with helium-4 proportional recoil counters. Rev. Sci. Instrum. **63**, 4536–4538 (1992). https://doi.org/10.1063/1.1143712
6. C.W. Barnes, H.S. Bosch, H.W. Hendel et al., Triton burnup measurements and calculations on TFTR. Nucl. Fusion **38**, 597–618 (1998). https://doi.org/10.1088/0029-5515/38/4/310
7. F.B. Marcus, J.M. Adams, B. Balet et al., Neutron emission profile measurements during the 1st tritium experiments at jet. Nucl. Fusion **33**, 1325–1344 (1993). https://doi.org/10.1088/0029-5515/33/9/i08
8. G. Nemtsev, V. Amosov, S. Meshchaninov et al., Study of the triton-burnup process in different JET scenarios using neutron monitor based on CVD diamond. Rev. Sci. Instrum. **87**, 11D835 (2016). https://doi.org/10.1063/1.4962190
9. W. Ullrich, H.S. Bosch, F. Hoenen, Application of a Si-diode detector for fusion product measurements in ASDEX Upgrade. Rev. Sci. Instrum. **68**, 4434–4438 (1997). https://doi.org/10.1063/1.1148410
10. J. Jo, M.S. Cheon, K.-J. Chung et al., Sample design and gamma-ray counting strategy of neutron activation system for triton burnup measurements in KSTAR. Fusion Eng. Des. **109–111**, 545–548 (2016). https://doi.org/10.1016/j.fusengdes.2016.02.058
11. J. Jo, M. Cheon, J.Y. Kim et al., Triton burnup measurements in KSTAR using a neutron activation system. Rev. Sci. Instrum. **87**, 11D828 (2016). https://doi.org/10.1063/1.4961273
12. J. Jo, M. Cheon, J. Kim et al., Initial operation results of NE213 scintillation detector for time-resolved measurements on triton burnup in KSTAR. Rev. Sci. Instrum. **89**, 10I118 (2018). https://doi.org/10.1063/1.5039308
13. S. Wu, An overview of the EAST project. Fusion Eng. Des. **82**, 463–471 (2007). https://doi.org/10.1016/j.fusengdes.2007.03.012
14. K. Li, L. Hu, G. Zhong et al., Development of neutron activation system on EAST. Rev. Sci. Instrum. **91**, 013503 (2020). https://doi.org/10.1063/1.5126746
15. B. Hong, G.Q. Zhong, L.Q. Hu et al., Diagnostic of fusion neutrons on EAST tokamak using 4H-SiC detector. IEEE Trans. Nucl. Sci. **69**, 639–644 (2022). https://doi.org/10.1109/tns.2022.3146180
16. G.A. Wurden, R.E. Chrien, C.W. Barnes et al., Scintillating-fiber 14 MeV neutron detector on TFTR during DT operation. Rev. Sci. Instrum. **66**, 901–903 (1995). https://doi.org/10.1063/1.1146200
17. T. Nishitani, M. Hoek, H. Harano et al., Triton burn-up study in JT-60U. Plasma Phys. Controlled Fusion **38**, 355–364 (1996). https://doi.org/10.1088/0741-3335/38/3/010
18. N. Pu, T. Nishitani, M. Isobe et al., Evaluation of scintillating-fiber detector response for 14 MeV neutron measurement.

J. Instrum. **14**, P10015 (2019). https://doi.org/10.1088/1748-0221/14/10/p10015
19. K. Ogawa, M. Isobe, T. Nishitani et al., Time-resolved triton burnup measurement using the scintillating fiber detector in the large helical device. Nucl. Fusion **58**, 034002 (2018). https://doi.org/10.1088/1741-4326/aaa585
20. N. Pu, T. Nishitani, K. Ogawa et al., Scintillating fiber detectors for time evolution measurement of the triton burnup on the large helical device. Rev. Sci. Instrum. **89**, 10I105 (2018). https://doi.org/10.1063/1.5035290
21. K. Ogawa, M. Isobe, S. Sangaroon et al., Time-resolved secondary triton burnup 14 MeV neutron measurement by a new scintillating fiber detector in middle total neutron emission ranges in deuterium large helical device plasma experiments. AAPPS Bull. **31**, 20 (2021). https://doi.org/10.1007/s43673-021-00023-2
22. T. Nishitani, M. Isobe, G.A. Wurden et al., Triton burnup measurements using scintillating fiber detectors on JT-60U. Fusion Eng. Des. **34–35**, 563–566 (1997). https://doi.org/10.1016/s0920-3796(96)00621-7
23. E. Takada, T. Amitani, A. Fujisaki et al., Design optimization of a fast-neutron detector with scintillating fibers for triton burnup experiments at fusion experimental devices. Rev. Sci. Instrum. **90**, 043503 (2019). https://doi.org/10.1063/1.5074131
24. K. Ogawa, M. Isobe, T. Nishitani et al., High detection efficiency scintillating fiber detector for time-resolved measurement of triton burnup 14 MeV neutron in deuterium plasma experiment. Rev. Sci. Instrum. **89**, 10I101 (2018). https://doi.org/10.1063/1.5032118
25. N. Pu, T. Nishitani, M. Isobe et al., Evaluation for gamma-ray rejection ability affecting neutron discrimination property in scintillating-fiber type of fast neutron detector. Nucl. Instrum. Method. Phys. Res. Sect. A **969**, 164000 (2020). https://doi.org/10.1016/j.nima.2020.164000
26. P. Hu, Z.G. Ma, K. Zhao et al., Development of gated fiber detectors for laser-induced strong electromagnetic pulse environments. Nucl. Sci. Tech. **32**, 58 (2021). https://doi.org/10.1007/s41365-021-00898-8
27. S. Zhang, J.S. Li, Y.J. Su et al., A method for sharing dynamic geometry information in studies on liquid-based detectors. Nucl. Sci. Tech. **32**, 21 (2021). https://doi.org/10.1007/s41365-021-00852-8
28. H. Cheng, B.H. Sun, L.H. Zhu et al., Intrinsic background radiation of $LaBr_3$(Ce) detector via coincidence measurements and simulations. Nucl. Sci. Tech. **31**, 99 (2020). https://doi.org/10.1007/s41365-020-00812-8
29. Y.J. Yao, C.J. Lin, L. Yang et al., The effects of beam drifts on elastic scattering measured by the large solid-angle covered detector array. Nucl. Sci. Tech. **32**, 14 (2021). https://doi.org/10.1007/s41365-021-00854-6
30. S. Agostinelli, J. Allison, K. Amako et al., Geant4—a simulation toolkit. Nucl. Instrum. Method. Phys. Res. Sect. A **506**, 250–303 (2003). https://doi.org/10.1016/s0168-9002(03)01368-8
31. QGSP_BIC_HP. https://geant4-userdoc.web.cern.ch/UsersGuides/PhysicsListGuide/html/reference_PL/QGSP_BERT.html
32. Optical Photon Processes in GEANT4. https://geant4.web.cern.ch/sites/default/files/geant4/collaboration/workshops/users2002/talks/lectures/OpticalPhoton.pdf
33. R.J. Zhou, G.Q. Zhong, L.Q. Hu et al., Development of gamma ray spectrometer with high energy and time resolutions on EAST tokamak. Rev. Sci. Instrum. **90**, 123510 (2019). https://doi.org/10.1063/1.5120843
34. Kuraray scintillation fiber. http://kuraraypsf.jp/psf/index.html
35. K. Ogawa, M. Isobe, H. Nuga et al., A study of beam ion and deuterium–deuterium fusion-born triton transports due to energetic particle-driven magnetohydrodynamic instability in the large helical device deuterium plasmas. Nucl. Fusion **61**, 096035 (2021). https://doi.org/10.1088/1741-4326/ac0d8a
36. E. Takada, A. Fujisaki, N. Nakada et al., Development of fast-neutron directional detector for fusion neutron profile monitor at LHD. Plasma Fusion Res. **11**, 2405020 (2016). https://doi.org/10.1585/pfr.11.2405020
37. Z. Cheng, Y. Yu, G. Li et al., Measurement of attenuation length and light yield of plastic scintillating fiber with silicon photomultiplier. At. Energy Sci. Technol. **54**, 340–347 (2020). https://doi.org/10.7538/yzk.2019.youxian.0221(inChinese)
38. I. Antcheva, M. Ballintijn, B. Bellenot et al., ROOT — A C++ framework for petabyte data storage, statistical analysis and visualization. Comput. Phys. Commun. **180**, 2499–2512 (2009). https://doi.org/10.1016/j.cpc.2009.08.005